

RADC-TR-88-217
Final Technical Report
October 1988



AD-A206 823

FD-TD SCATTERING FROM APERTURES

University of Kansas

Kenneth R. Demarest

APPROVED FOR PUBLIC RELEASE; DISTRIBUTION UNLIMITED.

ROME AIR DEVELOPMENT CENTER
Air Force Systems Command
Griffiss Air Force Base, NY 13441-5700

DTIC
ELECTE
APR 19 1989
S H D

This report has been reviewed by the RADC Public Affairs Division (PA) and is releasable to the National Technical Information Service (NTIS). At NTIS it will be releasable to the general public, including foreign nations.

RADC-TR-88-217 has been reviewed and is approved for publication.

APPROVED:



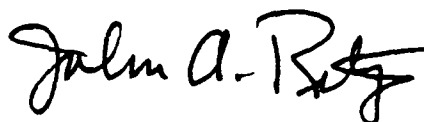
KEITH D. TROTT, CAPT, USAF
Project Engineer

APPROVED:



JOHN K. SCHINDLER
Acting Director of Electromagnetics

FOR THE COMMANDER:



JOHN A. RITZ
Directorate of Plans & Programs

If your address has changed or if you wish to be removed from the RADC mailing list, or if the addressee is no longer employed by your organization, please notify RADC (EECT) Hanscom AFB MA 01731-5000. This will assist us in maintaining a current mailing list.

Do not return copies of this report unless contractual obligations or notice on a specific document requires that it be returned.

UNCLASSIFIED

SECURITY CLASSIFICATION OF THIS PAGE

REPORT DOCUMENTATION PAGE				Form Approved OMB No. 0704-0188		
1a. REPORT SECURITY CLASSIFICATION UNCLASSIFIED			1b. RESTRICTIVE MARKINGS N/A			
2a. SECURITY CLASSIFICATION AUTHORITY N/A			3. DISTRIBUTION/AVAILABILITY OF REPORT Approved for public release; distribution unlimited.			
2b. DECLASSIFICATION/DOWNGRADING SCHEDULE N/A						
4. PERFORMING ORGANIZATION REPORT NUMBER(S) RSL Tech Report 5496-1			5. MONITORING ORGANIZATION REPORT NUMBER(S) RADC-TR-88-217			
6a. NAME OF PERFORMING ORGANIZATION University of Kansas		6b. OFFICE SYMBOL (If applicable)	7a. NAME OF MONITORING ORGANIZATION Rome Air Development Center (EECT)			
6c. ADDRESS (City, State, and ZIP Code) Radar Systems and Remote Sensing Lab 2291 Irving Hill Drive Lawrence KS 66045-2969			7b. ADDRESS (City, State, and ZIP Code) Hanscom AFB MA 01731-5000			
8a. NAME OF FUNDING/SPONSORING ORGANIZATION Rome Air Development Center		8b. OFFICE SYMBOL (If applicable) EECT	9. PROCUREMENT INSTRUMENT IDENTIFICATION NUMBER F30602-81-C-0205			
8c. ADDRESS (City, State, and ZIP Code) Hanscom AFB MA 01731-5000			10. SOURCE OF FUNDING NUMBERS			
			PROGRAM ELEMENT NO. 61102F	PROJECT NO. 2305	TASK NO. J4	WORK UNIT ACCESSION NO. P3
11. TITLE (Include Security Classification) FD-TD SCATTERING FROM APERTURES						
12. PERSONAL AUTHOR(S) Kenneth R. Demarest						
13a. TYPE OF REPORT Final		13b. TIME COVERED FROM Mar 87 TO Mar 88		14. DATE OF REPORT (Year, Month, Day) October 1988		
15. PAGE COUNT 36						
16. SUPPLEMENTARY NOTATION N/A						
17. COSATI CODES			18. SUBJECT TERMS (Continue on reverse if necessary and identify by block number)			
FIELD	GROUP	SUB-GROUP				
12	01		FDTD Numerical Methods ,			
20	14		Cracks , Scattering .			
			Gaps ,			
19. ABSTRACT (Continue on reverse if necessary and identify by block number)						
<p>This report studies the application of a popular numerical technique, the Finite-Difference Time-Domain (FDTD) technique to the problem of scattering by conductor-backed dielectric plates, with cracks in the dielectric. Although previous efforts have only dealt successfully with frequencies that are relatively high, the technique presented in this report is applicable at low frequencies (i.e., where the crack is small with respect to wavelength). The formalism presented requires a relatively minor change in the basic FDTD technique.</p> <p>The first section presents a brief overview of some electromagnetic numerical techniques as applied to dielectric structures. This is followed by an introductory section on the basics of the FDTD technique. Next, the FDTD technique is extended so that it can model thin dielectric sheets. This is followed by a discussion of the extension of the FDTD technique to conductor-backed dielectric sheets. Finally, the complete model of conductor-backed dielectric sheets with cracks is presented.</p>						
20. DISTRIBUTION/AVAILABILITY OF ABSTRACT <input type="checkbox"/> UNCLASSIFIED/UNLIMITED <input checked="" type="checkbox"/> SAME AS RPT. <input type="checkbox"/> DTIC USERS			21. ABSTRACT SECURITY CLASSIFICATION UNCLASSIFIED			
22a. NAME OF RESPONSIBLE INDIVIDUAL Keith R. Trott, Capt, USAF			22b. TELEPHONE (Include Area Code) (617) 377-4239		22c. OFFICE SYMBOL RADC (EECT)	

DD Form 1473, JUN 86

Previous editions are obsolete.

SECURITY CLASSIFICATION OF THIS PAGE

UNCLASSIFIED

CONTENTS

I. Introduction	1
II. General Comments on Numerical Techniques for Dielectric Scatterers	3
III. Review of FDTD	5
IV. Thin Dielectric Sheets	12
V. Conductor-Backed Dielectric Sheets	17
VI. Conductor-Backed Dielectric Slabs with Cracks	21
VII. Concluding Remarks	26
References	27



Accession For	
NTIS GRA&I	<input checked="" type="checkbox"/>
DTIC TAB	<input type="checkbox"/>
Unannounced	<input type="checkbox"/>
Justification	
By	
Distribution/	
Availability Codes	
Dist	Avail and/or Special
A-1	

I. INTRODUCTION

Recent advances in aircraft and radar technology have given rise to changes in aircraft construction and the emergence of new materials used in the construction of aircraft. One of these changes has been the introduction of dielectric structures for use both inside and outside the aircraft, replacing the metal structures traditionally used. The impetus for the use of these materials often stems from their desirable mechanical properties (strength, weight, etc.), but the desirability of aircraft with low radar cross sections has also enhanced their attractiveness.

The use of these dielectric structures in modern aircraft has introduced a new challenge in the area of the electromagnetic properties of aircraft that incorporate these new materials. These properties include the radar response of the aircraft, the performance of antennas mounted on them, and their response to threats such as Nuclear Electromagnetic Pulse (NEP) or lightning. Whereas the scattering characteristics of metal structures have been studied for many years and a great number of numerical techniques have been developed to calculate them, this is not true of dielectric scatterers. This is the result of two primary factors. First, in years past dielectrics were of minimal importance in structures such as aircraft. Thus, the relative neglect of dielectrics was natural. However, the second factor is that in most cases, Maxwell's equations are much more difficult to solve when dielectrics are involved. This is basically because fields penetrate dielectrics, whereas they are simply reflected from metals.

A dielectric structure currently used in aircraft that is of particular interest within the electromagnetic modeling community is the thin dielectric sheet. These structures can either be free standing (i.e., not layered) or layered (e.g., conductor-backed). Examples of the former are aerodynamic control surfaces such as fins. An example of the latter would be a fuselage constructed using conductor-backed, thin, dielectric panels. In either case, the electromagnetic modeling of these structures is more difficult than the corresponding metal structures since dielectrics are volume scatterers, as opposed to metal structures, which are surface scatterers.

This report studies the application of a popular numerical technique, the Finite-Difference Time-Domain (FDTD) technique to the problem of scattering by conductor-backed dielectric plates, with cracks in the dielectric. Although previous efforts have only dealt successfully with frequencies that are

relatively high, the technique presented in this report is applicable at low frequencies (i.e., where the crack is small with respect to wavelength). The formalism presented requires a relatively minor change in the basic FDTD technique.

The section to follow presents a brief overview of some electromagnetic numerical techniques as applied to dielectric structures. This is followed by an introductory section on the basics of the FDTD technique. Next the FDTD technique is extended so that it can model thin dielectric sheets. This is followed by a discussion of the extension of the FDTD technique to conductor-backed dielectric sheets. Finally, the complete model of conductor-backed dielectric sheets with cracks is presented.

II. GENERAL COMMENTS ON NUMERICAL TECHNIQUES FOR DIELECTRIC SCATTERERS

The numerical solution of Maxwell's equations has, of course, been a topic of great importance for many decades. As a result, there are a great number of techniques available for solving a wide range of problems of interest to the electromagnetic community. Included in the list of popular numerical techniques are integral equation methods, eigenvector methods, finite element methods, partial differential equation methods, asymptotic techniques, and radiative transfer methods, just to name a few. In spite of the seemingly large number of techniques available, it is often not particularly clear which method (if any) is well suited to a particular application. Certainly there is no one technique that is best suited to all situations.

As has been stated earlier, geometries containing dielectrics are particularly difficult to model since they are by nature volume, rather than surface, scatterers. This means that the unknown being searched for (usually a field or current distribution) exists not just on the surface of the scatterer, but also within. This obviously adds another dimension to the problem and thus increases both the computational and storage requirements of most numerical techniques.

The presence of slots or cracks in a dielectric scatterer poses a particularly difficult challenge since it combines two different problems: the volume scattering of the dielectric and the nonlinear field behavior near sharp discontinuities. In spite of the importance of this particular geometrical feature within electromagnetic engineering, little progress has been made in the analytical solution of such problems. One notable exception has been at high frequencies, where the Geometrical Theory of Diffraction¹ (GTD) can be used.

Two techniques that have enjoyed a great deal of popularity within the electromagnetic community are the Method of Moments² (MoM) and the Finite-Difference Time-Domain (FDTD) technique.³ Both techniques have proved very successful in a wide range of problems, and of course, both have their drawbacks. Basically, the MoM is an integral equation technique, usually thought of as operating in the frequency domain. With this technique, the unknown (generally a surface current or an interior field) is expanded in a finite dimensional basis and then a matrix equation is solved that minimizes the error (generally the boundary conditions) in the solution.

In the FDTD, Maxwell's equations are generally solved by direct integration in the time domain. Here, both time and space are divided into a numerical grid. The electric and magnetic fields are then advanced temporally by calculating the line integral of the previously calculated fields in each cell so as to obtain the time rate of change of each field component in each cell. In this way, time-marching solutions are obtained without the need to invert a matrix.

Although both of these techniques have been used with success to solve problems involving dielectrics, it has recently been shown⁴ that the FDTD has certain advantages over the MoM when dielectrics are involved. These advantages stem from an overall savings in the number of computer operations that need to be performed in order to solve problems of a given electrical size. The technique has been continually advanced in recent years so that a wide range of geometries can be modeled.^{5,6,7,8} It will be the subject of the subsequent sections to show how this technique can be augmented so that it can be used on thin dielectric structures with cracks.

III. REVIEW OF FDTD

The FDTD technique was first introduced for electromagnetic problems by Yee.³ To a large extent, this technique has been relatively unchanged since its introduction. The development in this section will be specialized to the case of simple conducting scatterers suspended in free space. This discussion will act as an introduction to those later sections that consider augmentations of this basic technique when dealing with scatterers containing thin dielectric sheets and the possibility of cracks.

Although Yee's original formulation of the technique was in terms of the differential form of Maxwell's equations (and hence the name FDTD), it has been shown⁸ that, in many instances, a superior view of the technique is obtained by starting with the integral form of Maxwell's equations and implementing them over small volumes of the solution space. Since it is this integral formulation that offers the most insight to the dielectric structures to be considered in the following sections of this report, the discussion to follow will be from this perspective.

Maxwell's equations can be stated in integral form as:

$$\oint \vec{H} \cdot d\vec{l} = I + \frac{\partial}{\partial t} \int \epsilon \vec{E} \cdot d\vec{s} \quad [1a]$$

$$\oint \vec{E} \cdot d\vec{l} = -\frac{\partial}{\partial t} \int \mu \vec{H} \cdot d\vec{s} \quad [1b]$$

For ease of reference, the first equation will often be referred to as Ampere's law, and the second, Faraday's law. As can easily be seen from these equations, a curling magnetic field causes a time-varying electric field, and vice versa. In fact, the development in time of an electromagnetic field can be thought of as the back and forth action and reaction between electric and magnetic fields. The FDTD exploits this very view of electromagnetic fields.

The FDTD approach proceeds to solve for the electric and magnetic fields resulting from a particular incident field (or source) interacting with a scatterer by dividing both time and space into a numerical grid. As shown in Figure 1, the space in the vicinity of the scatterer is divided into an array of rectangular cells. Within each cell, six components of the electric and magnetic fields are evaluated at distinct points in time. Figure 2 shows the points at which electric and magnetic fields are evaluated in each cell. It should be noticed that electric and magnetic fields are evaluated at

interlaced points in space. This interlacing has been deliberately engineered so as to readily calculate the line integral of the electric field about each magnetic field point, and vice versa. These fields are also evaluated at interlaced points in time.

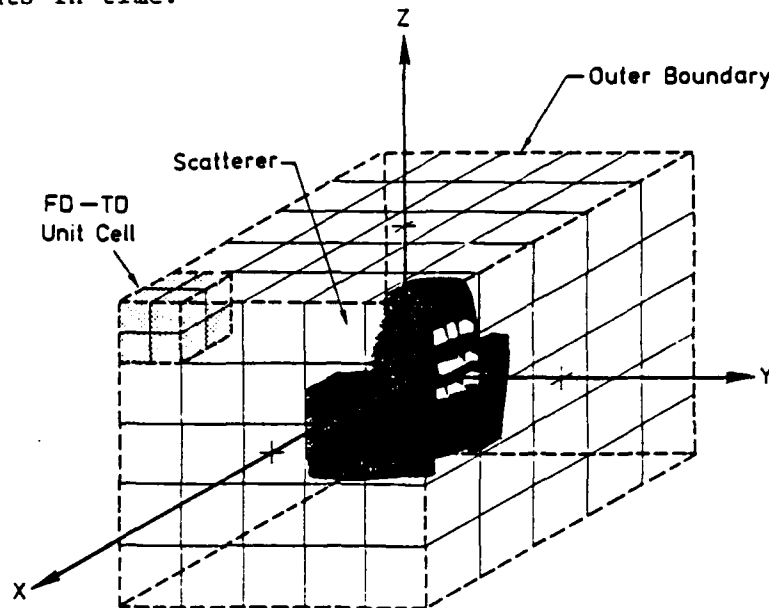


FIGURE 1. An arbitrary scatterer immersed in a rectangular FDTD numerical grid.

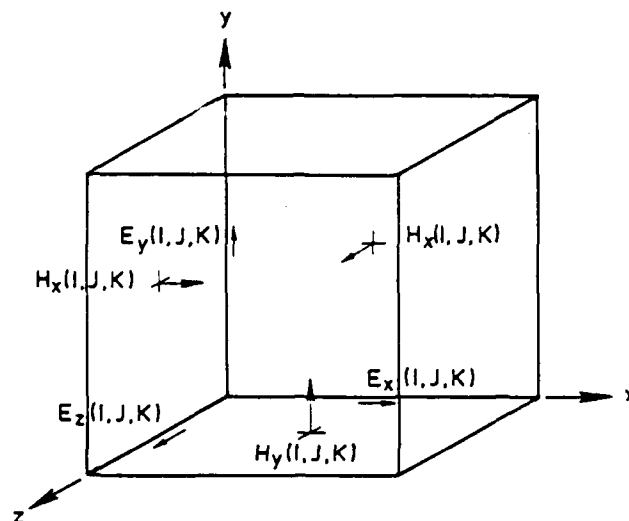


FIGURE 2. An FDTD unit cell showing the electric and magnetic field evaluation points

The FDTD technique begins the solution of the fields with the assumption that the system is starting from some known condition--most often an assumption of zero initial fields. Thus, it is assumed that the electric fields are known at each lattice point at $t = 0$, and the magnetic fields are also known at each lattice point at $t = \frac{-\Delta t}{2}$. Given this assumption, Faraday's law can be invoked along the three perpendicular paths in each cell to arrive at expressions of the form:

$$\oint_{C_1} \vec{E} \cdot d\vec{l} = \frac{-\partial}{\partial t} \int_{S_1} \mu(-H_x) dy dz \quad [2]$$

Here, the path of integration, C_1 , is counter clockwise around the perimeter of any cell (in this case in the $x = 0$ plane), and the surface S_1 is that which is enclosed by C_1 . This contour is depicted in Figure 3 (which shows a y - z plane cut of the three-dimensional lattice). In this figure, the electric and magnetic field evaluation points pertinent to Equation [2] are indicated. Also, Δy and Δz are the cell dimensions in the y and z directions, respectively.

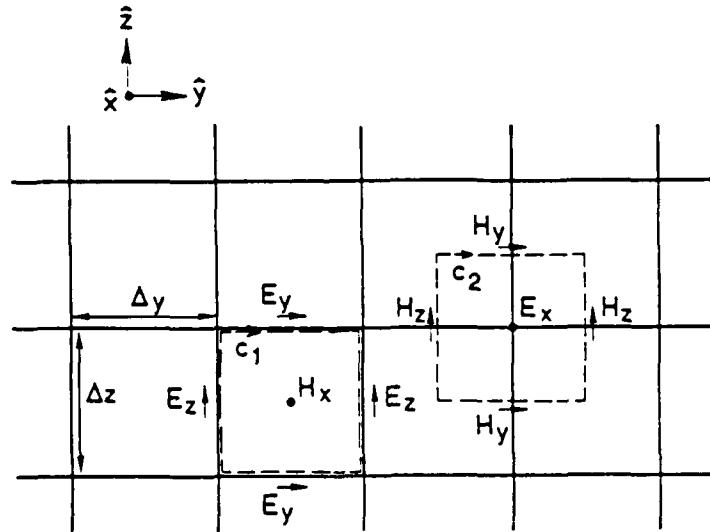


FIGURE 3. A planar cut of a 3-D FDTD grid showing the integral contours used for advancing the electric and magnetic fields in homogeneous regions.

If the cell in question contains only homogeneous media, the evaluation of Equation [2] proceeds by assuming that the dimensions of the cells are small enough (generally $\lambda/5$ or smaller) in each direction so that the fields within each cell can be considered to be linear functions of position. Considering

first the left side of Equation [2], it is seen that it consists of four separate line integrals. Restricting attention to the integral of E_z over the left-hand wall, we first assume that along this wall E_z varies as

$$E_z = EZ(I,J,K) + A \cdot z \quad , \quad [3]$$

where z is measured with respect to the center of the cell (i.e., the H_x evaluation point), and "A" is a constant. $EZ(I,J,K)$ is the value of E_z at the midpoint of the left wall (the indices I,J,K indicate that this field point is associated with the I,J,K'th cell). Thus, the contribution to the line integral of E_z along the left wall can be written as

$$\int_{\text{left wall}} E_z dz = EZ(I,J,K) \Delta z \quad . \quad [4]$$

A similar analysis can be performed on the other three legs of the line integral in the left side of Equation [2]. For instance, the integral along the right-hand path yields a result similar to Equation [4], except that the direction of integration is in the $-z$ direction and the center of this path coincides with the sample point $EZ(I,J+1,K)$. Also, the same type of assumption as shown in Equation [3] can be made for the y -directed electric fields along the upper and lower legs of the contour. Thus, the complete contour integral can be written as:

$$\oint_{C_1} \vec{E} \cdot d\vec{l} = [EZ^n(I,J,K) - EZ^n(I,J+1,K)]\Delta z \quad [5] \\ + [EY^n(I,J,K+1) - EY^n(I,J,K)]\Delta y \quad .$$

In this equation, the superscript n indicates that this line integral has been evaluated at time $t = n\Delta t$.

Turning attention to the right side of Equation [2], it is once again assumed that H_x is a linear function of position throughout the cell. Thus, H_x can be written as

$$H_x = HX(I,J,K) + A \cdot z + B \cdot y \quad . \quad [6]$$

Here the positions of y and z are measured with respect to the center of the

cell, and A and B are constants. Since this cell contains only homogeneous media, μ is constant throughout the cell and Equation [6] can be substituted into the right-hand side of Equation [2] to yield, after integration:

$$\frac{\partial}{\partial t} \int_{S_1} \mu (-H_x) dy dz = - \frac{\partial}{\partial t} \mu HX(I,J,K) \Delta y \Delta z \Big|_{t = n\Delta t}, \quad [7]$$

where $\Big|_{t = n\Delta t}$ indicates that the time derivative is to be performed at time $t = n\Delta t$.

The final step in evaluating the \bar{H} field at the center of this cell is to evaluate the time derivative in the above equation by standard central differencing. Thus:

$$\frac{\partial}{\partial t} \mu HX(I,J,K) \Delta y \Delta z \Big|_{t = n\Delta t} = \frac{\mu}{\Delta t} [HX^{n+1/2}(I,J,K) - HX^{n-1/2}(I,J,K)] \Delta y \Delta z, \quad [8]$$

where, as in the electric fields, the superscripts on HX indicate the times they are to be evaluated. Finally, substituting Equation [5] and [8] into Equation [2] and solving for $HX^{n+1/2}(I,J,K)$ yields

$$\begin{aligned} HX^{n+1/2}(I,J,K) = & HX^{n-1/2}(I,J,K) \\ & + \frac{\Delta t}{\mu} \left\{ \frac{1}{\Delta y} [EZ^n(I,J,K) - EZ^n(I,J+1,K)] \right. \\ & \left. + \frac{1}{\Delta z} [EY^n(I,J,K+1) - EY^n(I,J,K)] \right\}. \end{aligned} \quad [9]$$

This is the final FDTD expression for evaluating the \hat{x} -directed magnetic fields in each cell. Similar expressions can be developed for the y and z components.

Once the values of the magnetic fields at time $t = (n+1/2)\Delta t$ have been calculated in each cell, an application of Ampere's law in each cell will yield the electric fields at time $t = (n+1)\Delta t$. The procedure for evaluating the integrals follows the same general scheme, with the exception that the contour integrals are about \bar{H} field points, rather than \bar{E} field points, as can be seen in Figure 3 (see contour C_2). A representative expression for advancing an \hat{x} -directed electric field in a cell containing only homogeneous material and no currents is:

$$EX^{n+1}(I,J,K) = EX^n(I,J,K)$$

$$- \frac{\Delta t}{\epsilon} \left\{ \frac{1}{\Delta y} [HZ^{n+1/2}(I,J-1,K) - HZ^{n+1/2}(I,J,K)] \right. \\ \left. + \frac{1}{\Delta z} [HY^{n+1/2}(I,J,K) - HY^{n+1/2}(I,J,K-1)] \right\} \quad [10]$$

The general procedure of the FDTD technique is to sequentially evaluate the magnetic fields over the entire solution space, then the electric fields at the next half-time step. This process is repeated on and on. In this way, time-marching solutions are obtained.

The sources of the incident fields in the solution space can be specified in a variety of ways. If the source can be specified as a known current distribution relatively close to the source, the time history of these currents can be forced directly in Ampere's law (Equation [1a]). For sources distant from the scatterer, it is generally best to divide the total fields into incident and scattered components. Since the incident fields are assumed to be known over all of space for all time, the FDTD technique only needs to advance the scattered fields, noting that in cells containing free space they satisfy exactly the same Maxwell's equations as do the incident fields. It is also possible to have regions in the FDTD solution space where total fields are evaluated and stored, and other regions where only scattered fields are calculated.⁹ This scheme is popular when dielectric scatterers are present.

In cells containing perfectly conducting material, boundary conditions must be enforced. For those regions in which total fields are being calculated, the tangential electric fields at the conductor surfaces must be maintained at zero. For those regions in which scattered fields are being calculated, the appropriate condition is that the tangential components of the scattered fields must be maintained to equal the negative of the incident tangential fields. For this latter case, it can easily be seen that the scattered fields literally grow out of the scatterer since the scattered fields will not start until the incident field "hits" the scatterer. Only then will the calculated fields begin.

A final point to be mentioned here is the treatment of the fields along the edges of the solution space. The special problem here is that in order to continue to update the tangential electric fields along this boundary using the usual Ampere's law procedure, the values of magnetic fields beyond the

boundary would be required. If one proceeds blindly by ignoring this lack of information and tacitly assumes that these needed field components are zero, this will give rise to non-physical reflections and the numerical solution will be perturbed. To address this problem, several schemes have been developed whereby these needed fields are estimated from known values within the solution space. These techniques yield relatively small reflections, although work is being done to find even better estimators. The technique used by most current investigators (including this principal investigator) is that developed by Mur⁹ (usually the 2nd order solution).

IV. THIN DIELECTRIC SHEETS

The analysis of scatterers containing solid dielectric components is very straightforward. When dielectric material is present throughout cells in which total (as opposed to scattered) fields are being calculated, it is necessary only to change the constitutive parameters (i.e., μ , ϵ , and σ) within those cells.

In situations where a scatterer contains thin dielectric sheets one can, of course, use cell dimensions that are small enough to resolve the sheet as a collection of solid cells of dielectric. This, however, would generally require cell dimensions throughout the problem space at least as small as the dielectric sheet thickness, thus severely encumbering the technique both in computational time and storage when the sheet is very thin. To circumvent this undesirable situation, a scheme whereby the cell size can be allowed to be much larger than the slab thickness is desirable and will next be developed in the paragraphs to follow.

Figure 4 shows a two-dimensional cut of a FDTD spatial grid containing a thin dielectric sheet scatterer. The dielectric, of thickness d and permittivity ϵ , is represented by the shaded region. The electric and magnetic field sample points pertinent to this discussion are labeled in this figure.

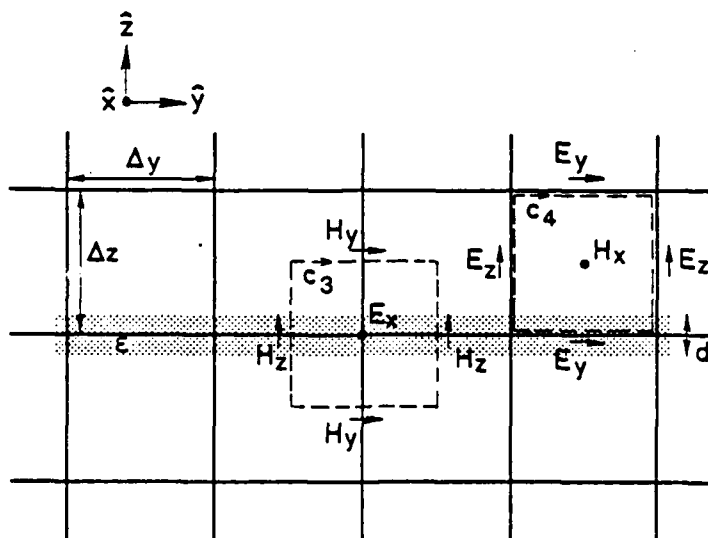


FIGURE 4. The orientation of a thin dielectric slab within the FDTD grid, showing the integration contours used to advance the electric and magnetic fields in the vicinity of the slab.

Viewing these field component locations in light of the field-advancing equations discussed in the previous section (Equations [1a] and [1b]), it can be seen that the only field components whose calculation will be directly affected by the presence of the slab are the tangential electric fields evaluated within the slab and the tangential magnetic field components just above and below the slab.

In order to use Ampere's and Faraday's laws (Equations [1a] and [1b], respectively) to calculate the tangential fields in the vicinity of the dielectric, some assumptions must be made concerning the behavior of these fields. To aid in this, observations were made of the fields in the vicinity of an electrically thin, infinite dielectric slab, subjected to a pulsed plane wave with various angles of incidence. It was found that the magnetic fields, although affected by the presence of the dielectric, maintain relatively linear behavior through the dielectric. As for the tangential electric fields, it is found that they too maintain relatively linear behaviors, with a small change in slope at the air/dielectric interface. The normal electric fields, as would be expected, exhibit a discontinuity at the air/dielectric interface of value equal to the ratio of the air and dielectric permittivities.

Given the above observations, it is reasonable to assume that, for thin slabs ($d \ll \lambda$), all magnetic fields and the tangential electric fields can be modeled as linear functions throughout those cells containing the slabs. On the other hand, the normal electric fields, which exhibit a definite discontinuity, must be modeled with this discontinuity built into the model in order for applications of Ampere's and Faraday's laws to provide meaningful results.

Turning attention to the evaluation of the tangential electric fields within the slab, it is noticed that the evaluation of the left side of Ampere's law around a contour such as C_3 will proceed just as in the "standard" FDTD technique since the magnetic fields are still assumed to be linear functions of position. The evaluation of the right side of Equation [1a] must, however, be modified since, although the electric field is assumed to be a linear function of position throughout the cell volume, ϵ is not. Taking this into account and integrating, one obtains:

$$EX^{n+1}(I,J,K) = EX^n(I,J,K)$$

$$- \frac{\Delta t}{\epsilon_0 + (\epsilon - \epsilon_0) \frac{d}{\Delta z}} \left\{ \frac{1}{\Delta y} [HZ^{n+1/2}(I,J-1,K) - HZ^{n+1/2}(I,J,K)] \right. \\ \left. + \frac{1}{\Delta z} [HY^{n+1/2}(I,J,K) - HY^{n+1/2}(I,J,K-1)] \right\} . \quad [11]$$

It should be noted that the above formula becomes the same as Equation [10] in the limit as $d \rightarrow 0$ or $\epsilon \rightarrow \epsilon_0$, as would be expected. Also, as d becomes larger (but still small with respect to wavelength) or ϵ becomes larger, the predicted value of $EX(I,J,K)$ becomes smaller. Again this is to be expected since the natural tendency of the slab to lower the electric field within it will become more dominant as the slab thickness or permittivity increases. A similar equation can be developed for E_y .

In order to advance the magnetic fields above and below the slab, Faraday's law (Equation [1b]) must be evaluated around a contour such as C_4 . There, the evaluation of the right side of Equation [1b] proceeds exactly as if the dielectric were not there since it has been assumed that the magnetic field has distributed itself linearly throughout these cells, just as in a free-space cell. On the other hand, the evaluation of the line integral of \vec{E} around the perimeter of the cell must be handled differently due to the discontinuity of the normal component of \vec{E} . Figure 5 depicts the behavior of E_z as a function of z in a cell that contains the dielectric slab. The function that describes this behavior is

$$EZ = \begin{cases} \frac{\epsilon_0}{\epsilon} [EZ(I,J,K) + A \cdot z] & -\frac{\Delta z}{2} < z < -\frac{\Delta z}{2} + \frac{d}{2} \\ EZ(I,J,K) + A \cdot z & -\frac{\Delta z}{2} + \frac{d}{2} < z < \frac{\Delta z}{2} \end{cases} , \quad [12]$$

where z is measured with respect to the center of contour C_4 .

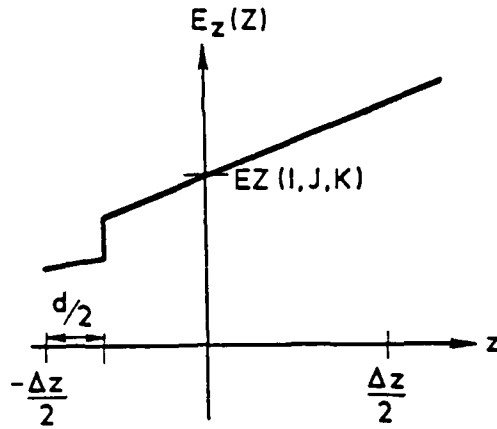


FIGURE 5. The assumed behavior along the z direction of the normal component of the electric field within the contour C_4 of FIGURE 4.

When integrating the electric field described by Equation [12] in the left-hand side of Faraday's law (Equation [1b]), it is seen that there exists an ambiguity since, although the value of $E_z(I,J,K)$ is assumed to be known for previous time steps and obtainable for future time steps, the slope, "A", is not. However, "A" can be estimated from the known values of E_z on both sides of the slab. Thus:

$$A(I,J) = \frac{1}{\Delta z} [E_z^n(I,J,K) - E_z^n(I,J,K-1)] \quad , \quad [13]$$

where $A(I,J)$ denotes the slope of E_z along the lattice lines $x = I \cdot \Delta x$ and $y = J \cdot \Delta y$. Substituting Equations [12] and [13] into Faraday's law and integrating around the contour C_4 yields:

$$\begin{aligned}
HX^{n+1/2}(I,J,K) = & HX^{n-1/2}(I,J,K) \\
& + \frac{\Delta t}{\Delta y \Delta z \mu} \left\{ \left[\Delta z + \frac{d}{2} \left(\frac{\epsilon_0}{\epsilon} - 1 \right) \right] [EZ^n(I,J,K) - EZ^n(I,J+1,K)] \right. \\
& + [A(I,J) - A(I,J+1)] \frac{d}{4} \left(\frac{\epsilon_0}{\epsilon} - 1 \right) \left(\frac{d}{2} - \Delta z \right) \\
& \left. + \Delta y [EY^n(I,J,K+1) - EY^n(I,J,K)] \right\} \quad .
\end{aligned} \tag{14}$$

A similar equation can be developed for H_y . If the slabs become thicker than $\lambda/5$, it is best to model them as solid cubes.

Equations [11] and [14] constitute the only modifications needed to allow the FDTD technique to model thin dielectric structures.

V. CONDUCTOR-BACKED DIELECTRIC SHEETS

The modeling of a thin dielectric slab backed by a vanishingly thin conducting sheet is, in some ways, easier than that of a dielectric slab. This is because the tangential electric and the normal magnetic fields at the dielectric/conductor interface are known (i.e., they are zero).

An FDTD model of a thin, conductor-backed dielectric sheet is shown in Figure 6. The dielectric sheet is shown as the shaded region, and the conducting sheet is shown as the solid line beneath it. A typical contour used to evaluate the tangential electric fields at the air/dielectric interface is shown as C_5 . Here, the contour is shortened in the z dimension as compared to "normal" contours due to the presence of the conducting sheet at the bottom of the contour. Ampere's law can be utilized along this contour to evaluate E_x along the air/dielectric interface if assumptions are made about the behavior of E_x and H_z within and along the contour, as well as the value of H_y along the conductor surface.

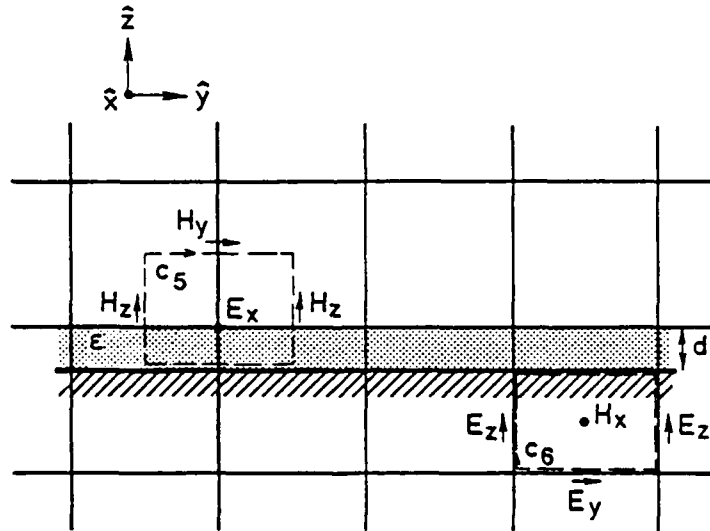


FIGURE 6. The orientation of a thin conductor-backed dielectric sheet within the FDTD grid, showing the integration contours used to evaluate tangential electric fields above the slab and magnetic fields below the slab.

Since both E_x and H_z have zero values at the conductor surface and will vary linearly near and within the dielectric, E_x and H_z can be modeled as:

$$H_z = \begin{cases} 0 & -\frac{\Delta z}{2} < z < -d \\ HZ(I,J,K) \left[1 + \frac{z}{d}\right] & -d < z < \frac{\Delta z}{2} \end{cases} \quad [15]$$

and

$$E_x = \begin{cases} 0 & -\frac{\Delta z}{2} < z < -d \\ EX(I,J,K) \left[1 + \frac{z}{d}\right] & -d < z < \frac{\Delta z}{2} \end{cases} \quad [16]$$

where $HZ(I,J,K)$ and $EX(I,J,K)$ represent the values of these fields at the air/dielectric interface. Also, z is measured with respect to the center of C_5 . Equations [15] and [16] are depicted in Figure 7.

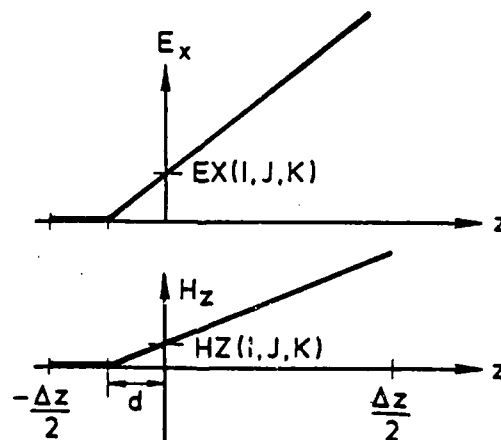


FIGURE 7. The assumed variations along the z direction of the tangential electric and normal magnetic fields within the contour C_5 of FIGURE 6.

Substituting Equations [15] and [16] into Ampere's law (Equation [1a]) and evaluating about contour C_5 yields:

$$EX^{n+1}(I,J,K) = EX^n(I,J,K)$$

$$- \frac{\Delta t}{[(\epsilon - \epsilon_0) \frac{d}{2} + \frac{\epsilon_0}{2d} (\frac{\Delta z}{2} + d)^2] \Delta y} \quad [17]$$

$$\left\{ \left[\frac{1}{2d} \left(\frac{\Delta z}{2} + d \right)^2 [HZ^{n+1/2}(I,J-1,K) - HZ^{n+1/2}(I,J,K)] \right. \right.$$

$$\left. \Delta y [HY^{n+1/2}(I,J,K) - H_{yc}^{n+1/2}] \right\} \quad .$$

In the above equation, H_{yc} is the \hat{y} directed magnetic field along the bottom of the contour. Note that this location does not coincide with any normal \bar{H} field evaluation points. This has occurred because the conducting sheet does not lie along a grid line. To evaluate this field, use will be made of the y component of the point form of Faraday's law:

$$\frac{\partial E_x}{\partial z} - \frac{\partial E_z}{\partial x} = -\mu \frac{\partial H_y}{\partial t} \quad . \quad [18]$$

In order to evaluate this expression at the conductor surface, the derivatives on the left side of the expression must be estimated. Of these, $\frac{\partial E_x}{\partial z}$ is the easiest to evaluate since the form of E_z has already been specified in Equation [16]. Thus, $\frac{\partial E_x}{\partial z}$ is given by

$$\frac{\partial E_x}{\partial z} = \frac{1}{d} EX(I,J,K) \quad . \quad [19]$$

In evaluating the term $\frac{\partial E_z}{\partial x}$, it is noticed that the form of E_z has not (and cannot) be as easily specified as was E_x since an electric field normal to a conducting surface need not have zero value at that surface. It must, however, approach that surface with zero slope. Thus, it will be assumed that the values of E_z at a distance of $d + \frac{\Delta z}{2}$ above the ground plane are sufficient to predict $\frac{\partial E_z}{\partial x}$ at the conductor surface. Thus, we have:

$$\frac{\partial E_z}{\partial x} = \frac{\epsilon_0}{\epsilon \Delta x} [EZ(I+1, J, K) - EZ(I, J, K)] \quad . \quad [20]$$

Note that the $\frac{\epsilon_0}{\epsilon}$ multiplier in the above expression arises from the known discontinuity in E_z across the air/dielectric interface. Equations [19] and [20] can now be substituted into Equation [18] to yield

$$H_{yc}^{n+1/2} = H_{yc}^{n-1/2} - \frac{\Delta t}{\mu} \left[\frac{1}{d} EX^n(I, J, K) - \frac{\epsilon_0}{\epsilon \Delta x} [EZ^n(I+1, J, K) - EZ^n(I, J, K)] \right] \quad . \quad [21]$$

This is the value of H_{yc} as intended for use in Equation [17] to evaluate the tangential electric fields at the air/dielectric interface. Note that in order to evaluate Equation [21], the value of H_{yc} at the previous time step must be stored. This means that computer storage must be reserved for these tangential magnetic fields all along the conducting sheet.

The evaluation of H_z at the air/dielectric interface needs no special attention since the integration takes place for a fixed value of z and the fields H_z and E_x and E_y are continuous across this interface. Thus, since the variables EX and EY represent the values of the field at the interface, the usual calculation of Faraday's law will naturally yield the value of H_z at this interface. As an important example, for the case where $d = 0$, Equation [16] will yield zero values of both tangential components of \vec{E} and thus zero values of H_z .

Finally, the expressions for updating the tangential magnetic field components (H_x and H_y) below the conductor must be slightly modified to reflect the fact that the conductor sheet is protruding into the cells under the slab. In evaluating Faraday's law around the contour C_6 (see Figure 6), it is of course noticed that the point at which H_x is to be evaluated is not in the center of the contour, giving rise to an ambiguity in its value since the slope of H_x at that point cannot be exactly known. Fortunately, since this point is close to a perfectly conducting surface, the slope of H_x with respect to z will be small and thus relatively unimportant. Thus, the algorithm for calculating H_x needs only be modified by noting that the surface area of the surface surrounded by C_6 is smaller by the linear multiplier $(1 - \frac{2d}{\Delta z})$.

VI. CONDUCTOR-BACKED DIELECTRIC SLABS WITH CRACKS

The problem of modeling a conductor-backed dielectric slab with a thin crack in the dielectric presents a modeling challenge when using any electromagnetic technique, and the FDTD is no exception. This difficulty arises from the relatively complex field distributions in the vicinity of the crack. These fields exhibit a relatively severe localized perturbation from their relatively smooth behavior away from the crack due to the collection of bound charges across the crack. These bound-charge distributions may be thought of as arising from the disruption of the bound currents flowing within the dielectric, since the crack presents an open circuit to these currents.

A FDTD model of a conductor-backed dielectric slab with a long, narrow crack is shown in Figure 8. Here, it is assumed that the air/dielectric interface lies along a grid coordinate axis, and the conductor lies below at a depth d ($d < \frac{\Delta z}{2}$). The crack is assumed to be a "clean" cut in the dielectric, of width w ($w < \frac{\Delta y}{2}$), and extends through to the conductor. It is further assumed that the crack runs out of the page and is aligned such that it appears in between grid lattice points. This alignment is such that the top of the crack coincides with an evaluation point for E_y . This particular

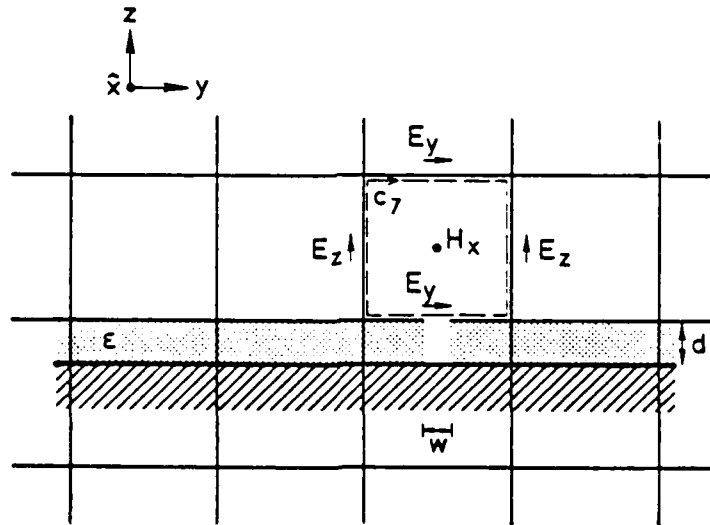


FIGURE 8. The orientation of a thin, conductor-backed dielectric slab with a long, narrow crack in the FDTD grid, showing the position of the crack with respect to the integration contour, C_7 , used to advance the tangential magnetic fields along the crack.

orientation of the crack within the FDTD lattice has been chosen so that the effect of the crack can be most accurately modeled for situations where the incident field produces strong fields across the crack (i.e., the dominant scattering mode of a crack).

Since the dielectric is assumed to be non-magnetic, it can be assumed that the magnetic field in its vicinity vary linearly throughout each cell. On the other hand, this assumption cannot be made about the tangential electric field in the vicinity of the crack since it would be expected that this field component will be enhanced inside the crack and exhibit a distribution similar to a static dipole in the vicinity of the crack, particularly within the crack and just above it. This gives rise to two difficulties. First, the nonlinear behavior will change the way that the right-hand side of Ampere's law (Equation [1a]) is evaluated to calculate the field at the lattice point given a knowledge of its surface integral. A second difficulty stems from the fact that it is not the value of $E_y(I,J,K)$ at the lattice point that is needed in Faraday's law when updating magnetic fields, but rather its average over the length of its respective cell wall. Thus, the nonlinear behavior of E_y along the \hat{y} direction must also be correctly modeled in order to accurately calculate the magnetic fields.

The way in which this nonlinear behavior of E_y above and within the crack is modeled presents the most challenging aspect of this problem. As is typical in FDTD analysis, there are a number of ways in which this could be accomplished. In the paragraphs to follow, the method that appears to show the most promise will be presented.

Since the crack is assumed to be narrow, the capacitance across the gap will be quite high. Thus, the polarization current flow in the dielectric

$$(\bar{J}_p = (\epsilon - \epsilon_0) \frac{\partial \bar{E}}{\partial t}) \text{ will be relatively unaffected on either side of the crack.}^\dagger$$

Given this, the crack can be thought of as perturbing the fields of a continuous dielectric slab by subtracting from the total polarization current in the

[†] Two physical explanations can be offered to support this claim. The first is that replacing a section of wire with a large capacitor will have little effect on the current in the rest of the circuit. The second is that the electric field in the air gap between the plates of a capacitor is only marginally affected when a thin dielectric (much thinner than the air gap) is added between the plates.

dielectric that which is no longer present in the crack. This suggests defining the total electric field in the vicinity of the crack as:

$$\bar{E} = \bar{E}_d - \bar{E}_p, \quad [22]$$

where \bar{E}_d is the electric field without the crack perturbation (which will henceforth be called the unperturbed field component), and \bar{E}_p is the electric field radiated by the missing polarization currents above the ground plane (but not in the presence of the dielectric). The logical sequence of Equation [22] is depicted in Figure 9.

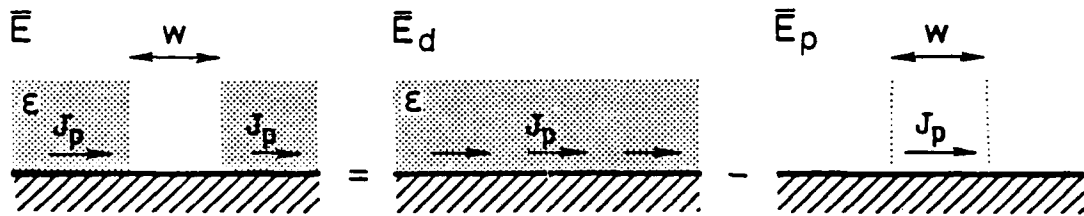


FIGURE 9. The physical representation of Equation [22], whereby the fields due to the long, narrow crack in a conductor-backed dielectric sheet are approximated as those with no crack present, minus the fields of the "missing" polarization currents.

The reason why the above scheme is attractive is that the field \bar{E}_d can be calculated by the usual conductor-backed dielectric formulas (Equation [17]), and \bar{E}_p can be calculated from the well-known field properties of short elements of current. Also, in the near field of a short current element the electric field is proportional to the time integral of the current.¹⁰ Thus, we can write:

$$\bar{E}_p = \int [J_{p_y} \bar{F}^y(y) + J_{p_z} \bar{F}^z(y)] dt, \quad [23]$$

where $\bar{F}^y(y)$ and $\bar{F}^z(y)$ are the near field pattern functions along the

\hat{y} direction of short current dipoles oriented in the \hat{y} and \hat{z} directions, respectively. J_{p_y} and J_{p_z} are the y and z components of the missing polarization currents, respectively. However, since $\bar{J}_p = (\epsilon - \epsilon_0) \frac{\partial \bar{E}_d}{\partial t}$, E_p can be written as:

$$\bar{E}_p = (\epsilon - \epsilon_0) E_{d_y} \bar{F}^y(y) + (\epsilon - \epsilon_0) E_{d_z} \bar{F}^z(y), \quad [24]$$

where E_{d_y} and E_{d_z} are the \hat{y} - and \hat{z} -directed unperturbed electric fields within the crack.

Knowing the relationship between the fields radiated by the "missing" polarization currents in the dielectric crack and the relatively unperturbed fields within the dielectric on either side of the crack, one can obtain the following expression for the \hat{y} -directed electric field by substituting Equation [24] into Equation [22]:

$$E_y = (E_{d_y} + A \cdot y) - E_{d_y} F_y^y(y) - E_{d_z} F_y^z(y), \quad [25]$$

where $F_y^y(y)$ and $F_y^z(y)$ are the y components of the pattern functions along the y coordinate due to \hat{y} - and \hat{z} -directed polarization currents, respectively, and "A" is a constant. Notice in this equation that the first term is a linear function of y , but the remaining two terms are nonlinear dipole fields.

Now that the electric field along the air/dielectric interface in the vicinity of the crack has been described in Equation [25], the line integral of Faraday's law (Equation [1b]) can now be evaluated. Looking at Equation [25], it is obvious that the line integral of the first term will be trivial since this field component varies linearly along the path. The integrals of the remaining two terms will be more challenging.

One approximation of these integrals could be obtained by lumping all of the missing polarization currents at the center of the crack. This assumption would yield simple expressions for the line integral of these terms. It may, however, be necessary to consider these currents as the volume currents which they truly are (i.e., they are functions of depth into the crack). If this

is the case, the integration of these terms will be more complex. In either case, however, it must be remembered that the fields of a short current are relatively simple, so these integrals need not be particularly complex.

Summarizing, this section has proposed a simple model of the behavior of the tangential electric field in the vicinity of a crack in a conductor-backed dielectric slab that can be calculated in terms of variables readily available from the FDTD technique for conductor-backed dielectric slabs. From this model of the electric field behavior, a technique for evaluating the magnetic fields above the air/dielectric interface has been proposed. Since the dipole nature of the fields in the vicinity of the crack are built into this technique, it is expected to be capable of accurately modeling the backscatter from such cracks.

VII. CONCLUDING REMARKS

This report has concerned itself with the development of a numerical technique capable of calculating the backscatter from dielectric slabs, with and without cracks. This work represents an extension of the well-known and popular FDTD technique, which, if not modified, is not well suited to geometries with fine detail (e.g., thin dielectrics or cracks).

In the case of dielectric slabs (with or without conductor backing), algorithms have been developed for direct insertion into any standard FDTD code. These algorithms are similar in form to the "standard" field-advancing equations in FDTD codes, but allow for the change in ϵ at the air/dielectric interface and the discontinuity of the normal electric field components at the interface. They are suited for situations in which the dielectric slab is small with respect to wavelength and the cell dimensions. Initial calculations from these formulas indicate that they are indeed capable of advancing the fields in the presence of these scatterers, although full-scale numerical testing will be the subject of follow-up efforts.

The analysis of conductor-backed dielectric structures with thin cracks presented in this report has identified the special modeling challenges of this geometry. The formalism developed followed from a perturbational analysis of the crack under the assumption that the presence of a thin crack has little effect on the electric fields (thus the polarization currents) inside the dielectric on either side of the crack. This assumption, along with the known radiating properties of small current filaments, yields a set of equations that depend on the fields of the dielectric without the crack. The best way of evaluating the spatial integrals in these formulas will again be the subject of follow-up work.

REFERENCES

1. R.G. Kouyoumjian, "The Geometrical Theory of Diffraction and Its applications," in Numerical and Asymptotic Techniques in Electromagnetics, R. Mittra, ed., Springer-Verlag, New York, 1975.
2. R.F. Harrington, Field Computation by Moment Methods, MacMillan, New York, 1968.
3. K.S. Yee, "Numerical Solution of Initial Boundary Value Problems Involving Maxwell's Equations in Isotropic Media," IEEE Transactions on Antennas and Propagation, Vol AP-14, No. 3, pp. 302-307, May 1966.
4. D.T. Borup, D.M. Sullivan, O.P. Gandhi, "Comparison of the FFT Conjugate Gradient Method and the Finite-Difference Time-Domain Method for the 2-D Absorption Problem," IEEE Transactions on Microwave Theory and Techniques, Vol. MTT-35, No. 4, pp. 383-395, April 1987.
5. K.S. Kunz and L. Simpson, "A Technique for Increasing the Resolution of Finite-Difference Solutions of the Maxwell Equation," IEEE Transactions on Electromagnetic Compatibility, Vol. EMC-23, No. 4, pp. 419-422, November 1981.
6. K.R. Demarest, "A Finite Difference-Time Domain Technique for Modeling Narrow Apertures in Conducting Scatterers," IEEE Transactions on Antennas and Propagation, Vol. AP-35, No. 7, pp 826-831, July 1987.
7. R. Holland, L. Simpson, "Finite-Difference Analysis of EMP Coupling to Thin Struts and Wires," IEEE Transactions on Electromagnetic Compatibility, Vol. EMC-23, No. 2, pp. 88-97, May 1982.
8. A. Taflove, K.R. Umashankar, B. Beker, F. Harfoush, "Detailed FD-TD Analysis of Electromagnetic Fields Penetrating Narrow Slots and Lapped Joints in Thick Conducting Screens," Accepted for publication in IEEE Transactions on Antennas and Propagation.
9. G. Mur, "Absorbing Boundary Conditions for the Finite-Difference Approximation of the Time-Domain Electromagnetic Field Equations," IEEE Transactions on Electromagnetic Compatibility, Vol. EMC-23, No. 4, pp. 377-382, Nov. 1981.
10. C.A. Balanis, Antenna Theory, Harper and Row Publishers, 1982, p. 103.



MISSION of Rome Air Development Center

RADC plans and executes research, development, test and selected acquisition programs in support of Command, Control, Communications and Intelligence (C³I) activities. Technical and engineering support within areas of competence is provided to ESD Program Offices (POs) and other ESD elements to perform effective acquisition of C³I systems. The areas of technical competence include communications, command and control, battle management, information processing, surveillance sensors, intelligence data collection and handling, solid state sciences, electromagnetics, and propagation, and electronic, maintainability, and compatibility.